Int J Adv Manuf Technol (2017) 91:445–452
DOI 10.1007/s00170-016-9655-4

ORIGINAL ARTICLE

Manufacturing of metallic micro-components using hybrid soft lithography and micro-electrical discharge machining

Khamis Essa[1] · **Francesco Modica**[2] · **Mohamed Imbaby**[3,4] · **Mahmoud Ahmed El-Sayed**[5] · **Amr ElShaer**[6] · **Kyle Jiang**[1] · **Hany Hassanin**[7]

Received: 10 July 2016 / Accepted: 18 October 2016 / Published online: 22 November 2016

Abstract In spite of significant improvements in micro-replication techniques, methods to fabricate well-defined net shape microstructures are still in a developing stage. Soft lithography has the capability to manufacture complex micro- and nanostructures. Although it is considered a robust technique, a major limitation is related to the distortion encountered in the fabricated structures during the drying process. In the present work, a manufacturing technology has been developed that emerges the benefits of soft lithography and micro-electrical discharge machining (μ-EDM) to produce stainless steel precise micro-components for micro-implantable devices. The micro-parts produced by soft lithography were subsequently surface processed via μ-EDM in order to improve the surface quality. In addition to this, it was found that μ-EDM drastically improved the surface roughness of stainless steel micro-components from Ra = 3.4 μm to Ra = 0.43 μm.

Keywords MEMS · EDM · Micro-machining · Soft lithography

✉ Hany Hassanin
h.hassanin@kingston.ac.uk; enghanisalama@yahoo.com

[1] School of Engineering, The University of Birmingham, Edgbaston, Birmingham, UK

[2] ITIA-CNR, Institute of Industrial Technologies and Automation, Bari, Italy

[3] Jubail University College, PO Box 10074, Jubail, Kingdom of Saudi Arabia

[4] Faculty of Engineering, Helwan University, PO Box 11718, Cairo, Egypt

[5] Department of Industrial and Management Engineering, Arab Academy for Science and Technology and Maritime Transport, Abu Qir, PO Box 1029, Alexandria 21599, Egypt

[6] Drug Discovery, Delivery and Patient Care (DDDPC), School of Life Sciences, Pharmacy and Chemistry, Kingston University London, Kingston Upon Thames, Surrey KT1 2EE, UK

[7] School of Mechanical and Aerospace Engineering, Kingston University, London SW15 3DW, UK

1 Introduction

The development of micro-fabrication through the past years has led to a diversity of miniaturized systems. Micro-electro-mechanical Systems (MEMS) can vary from relatively simple patterns to highly complex systems [1, 2]. This has been supported by the increase in the global market of MEMS devices. The global market for MEMS devices and production equipment was worth $11.7 billion in 2014. This market is expected to hit $21.9 billion by 2020 [3]. The application of micro-manufacturing technologies to biomedical engineering has introduced a novel generation of small devices that helped in both medical research and treatment. Lab on a chip and micro-implant systems allowed the reduction in power consumption, electronic noise and system complexity and capability.

Materials used in these systems must be biocompatible and able to work in vivo. Popular examples of biocompatible materials include silicon, polymers and glass. Although metals do not exhibit similar advantages as silicon concerning the functional properties, they are widely used in MEMS fabrication. Commonly used metals include gold, nickel, aluminium, stainless steel, copper, chromium, titanium, tungsten, platinum and silver [1, 4–8]. This is because metals exhibit high strength, which minimizes the possibility of experiencing major failures. Therefore, they have been the main choice of hermetic seals of large biomedical implants such as pacemakers [9–11].

Micro-fabrication methods used for metallic MEMS components generally have their origins to the conventional precision machining methods or silicon-based micro-machining. The methods are improved to suit the machined metal properties and the desired surface finish of the micro-component. X-ray lithography is a conventional micro-fabrication technique, which is suitable to fabricate polymeric and silicon-based materials. Another fabrication technique that is originated from X-ray lithography is the LIGA process. The LIGA is an acronym of a German word for lithography, electroforming and moulding. In this process, high aspect ratios could be achieved based on the combination of synchrotron radiation lithography and galvanoforming [12–18]. Laser micro-machining is a non-lithographic fabrication process, in which a laser beam is emitted in narrow and well-defined wavelengths with high power that can remove materials such as fine particles and vapour from a substrate. The process is capable of producing a wide range of material micro-components. However, it produces some problems in the micro-features such as the induced stress and heat-affected zone. In addition, the structures produced usually have rough edges. Focus ion beam (FIB) is a micro-milling technique that uses an ion beam to hit the surface of the sample causing the sputtering of a small amount of material in the form of ions or neutral atoms. Due to the removal of the material in the form of atoms or ions, the material removal rate is quite low [19, 20].

Stainless steel 316L is one of the most common metals in biomedical devices. This alloy has excellent biocompatibility and superior mechanical properties such as high mechanical strength, good ductility and excellent corrosion resistance. These properties make it an excellent candidate for micro-medical and micro-implant applications [12]. Soft lithography is a robust micro-fabrication technique. It provides a convenient, effective and low-cost method for the formation and manufacturing of micro- and nanostructures, with a feature size approaching 180 nm [20]. The process starts with the fabrication of a master mould. A soft elastomeric mould is then fabricated with the inverse of the master mould. Afterward, the soft mould is filled with the material slurry. Finally, the green pattern is demoulded and sintered. Soft lithography offers several advantages over traditional photolithography in the field of micro-fabrication. The process is less sensitive to surface topography than photolithography and could be used for a wide range of materials including stainless steel. The process was successfully used for many of chemically and physically sensitive materials such as dyes and biomolecules [21, 22]. Due to the potential of soft lithography, many researchers have utilized the technique to produce patterned structures. Schönholzer and Gauckler [23] proposed a process to fabricate ceramic microstructures in the range of several micrometers using soft lithography. They studied the influence of particle sizes on the pattern resolution of the ceramic component. In another research, Kim and his colleagues [24] reported the possibility of the fabrication of 3D free-standing micro-components using Al and Cu micro- and nano-powders. The authors suggested that considering some adjustments of the process, there is an opportunity of expanding this technology for many of the metallic micro-components. In additions, Zhigang et al. [25] fabricated monolithic alumina precision micro-components using polydimethylsiloxane (PDMS) soft mould filled with an aqueous suspension. Recently, Kahraman and co-researchers utilized a nanosphere soft lithography technique in the manufacturing of planar 3D metallic nano-void substrates suitable for surface-enhanced Raman spectroscopy (SERS) applications [26].

Although soft lithography is considered a productive and cheap process when compared to many other techniques, some problems exist in applying this technique, which affect the properties of the resultant micro-parts. One of the important problems of soft lithography is the distortion due to the uneven drying of the slurry. Soft lithography exhibits large and uneven shrinkage during drying and sintering processes and hence topographical distortions develop [27, 28]. In an attempt to improve the surface quality, Hassanin et al. used a slip casting technique in the manufacturing of the micro-parts. This helped to solve the problems arisen from the uneven drying of the micro-mould and significantly improved the surface quality of the resulting micro-component [12, 29].

In this study, micro-electrical discharge machining (μ-EDM) was applied to improve the surface roughness and the flatness of soft lithography products and in turn enhance their quality. μ-EDM is a thermo-electric process that uses electrical discharges to erode electrically conductive materials by a series of discrete sparks between the workpiece and the tool electrode, both submerged in a dielectric fluid. When the tool comes close enough to the workpiece, the dielectric medium that is initially non-conductive breaks down and becomes conductive and spark would be generated. The thermal energy released continuously and effectively removes the workpiece material by melting and evaporation [30–32]. The process is quite capable of machining intricate profiles from any electrical conductive material irrespective of its hardness and strength. By precisely controlling the amount energy released, it is possible to machine micro-features on any electrically conductive material. It was reported that high machining accuracy of micro-components that are smaller than 100 μm and a surface roughness of a fraction of a micrometer could be achieved using μ-EDM [33, 34].

Bigot et al. [35] performed a study on the optimization of μ-EDM parameters for rough and fine machining. They managed to optimize the EDM machining parameters to get the best surface quality and the maximum material removal rate. Mustafa et al. [36] used grey relational analysis method to optimize the process parameters during the machining of Inconel 718 super alloy. They studied the influence of μ-

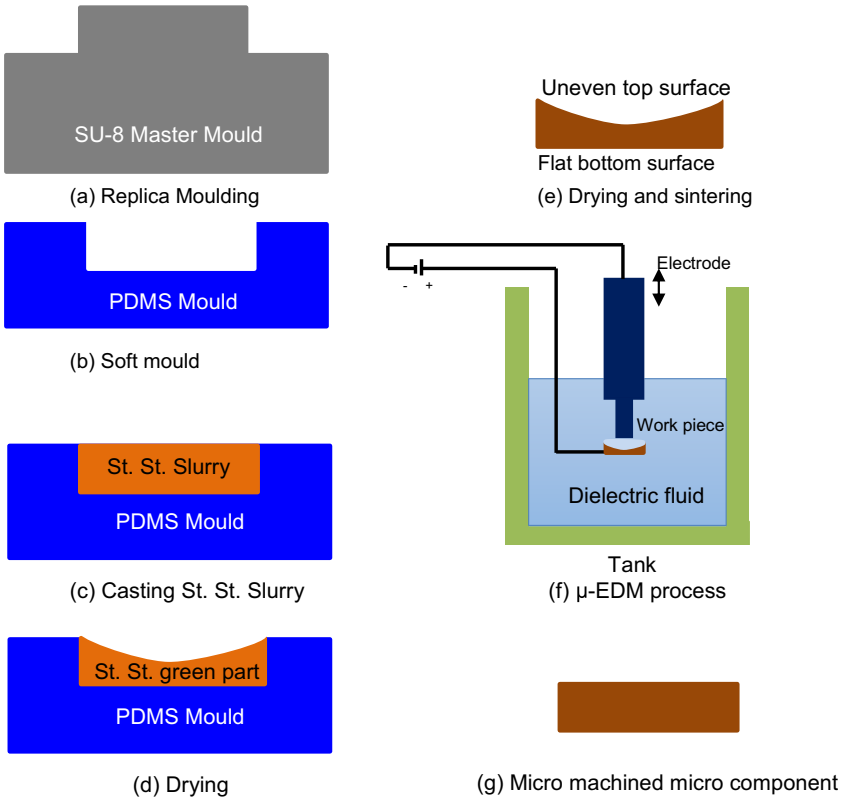

Fig. 1 Schematic diagram of the proposed hybrid soft lithography/ μ-EDM process: (a) Replica Moulding, (b) Soft mould, (c) Casting St. St. Slurry, (d)Drying, (e) Drying and sintering, (f) μ-EDM process, (g) Micro machined micro component

EDM process parameters such as pulse on time and peak current on machining characteristic of the samples. In addition, Luo and Chen were able to obtain samples with surface roughness of Ra = 0.04 μm by investigating the influence of pulse electromagnetic field during finishing EDM [37]. As described, EDM is a well-established machining method to achieve high quality surfaces. However, there are no reports found in using this technology to improve the surface quality of micro-parts fabricated using soft lithography.

The aim of this work is to introduce a hybrid micro-fabrication technology combines both the design freedom and robustness of soft lithography and the machining accuracy of μ-EDM to manufacture high quality micro-implant stainless steel parts. Stainless steel micro-gears with a pitch diameter of 2.5 mm and a minimum feature of 75 μm were first fabricated using soft lithography. Then μ-EDM was optimized to improve the surface roughness and the flatness of the components. The effect of μ-EDM parameters on the resulting surface roughness was also explored.

2 Experimental

Figure 1 illustrates the procedure to fabricate the stainless steel micro-parts using the proposed hybrid process. As shown in Fig. 1a, first, a master mould was manufactured. The master mould consisted of SU-8 micro-gears having a pitch diameter of 2.5 mm, a thickness of 1 mm, a minimum micro-feature of 75 μm and 27 teeth. The master mould was fabricated by pouring SU-8 onto a 4-in. silicon wafer. The wafer was then left for 20 min to flatten.

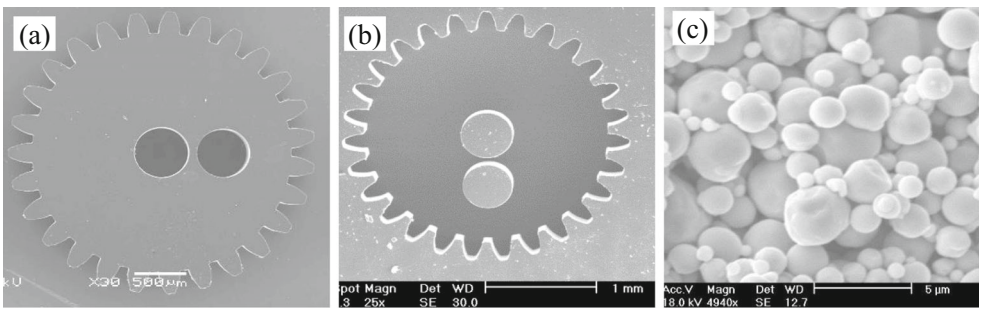

Fig. 2 **a** SU-8 master mould, **b** PDMS soft mould and **c** the as-received stainless steel powder

Table 1 The chemical compositions of the as-received 316-L powders (wt%)

As-received powder	Chemical composition					
	Fe	Cr	Ni	Mo	Mn	Others
Percentage	68	16.5	10.5	2.1	1.45	0.88

Afterward, the wafer was prebaked at 65 °C for 2 h and then at 95 °C for 30 h. The coated wafer was then exposed to a UV light with an energy density of 2.5 J cm^{-2} in a Canon PLA-501 FA UV-mask aligner. Afterwards, the post-exposure bake was carried out at 65 °C for 15 min and then at 95 °C for 25 min. Finally, the exposed wafer was immersed in EC solvent (Chestech, UK) for 1.5 h for development (Fig. 2a). The soft mould has been fabricated using a mixture of Sylgard 184 kit (Dow Corning, Midland, USA) with a ratio of 10:1 between the prepolymer and curing agent (Fig. 1b). The mixture was poured onto the master mould. The PDMS mixture was de-aired in a vacuum chamber to remove air bubbles and then was cured in an oven at 75 °C for 2 h. After cooling down, the soft mould was peeled off from the master mould, Fig. 2b. Details of the fabrication process of the master and soft moulds are presented in the literatures [8, 12, 29]. Stainless steel 316L micro-powder was supplied from Sandvik Osprey, UK. The particle size distribution was D10 = 1.1 μm, D50 = 1.8 μm and D90 = 3.6 μm. The chemical composition is listed in Table 1. The powder morphology was investigated under an SEM and is shown in Fig. 2c. As shown, the particles have spherical shapes with different sizes, which help forming homogeneous slurry and produce good density packing.

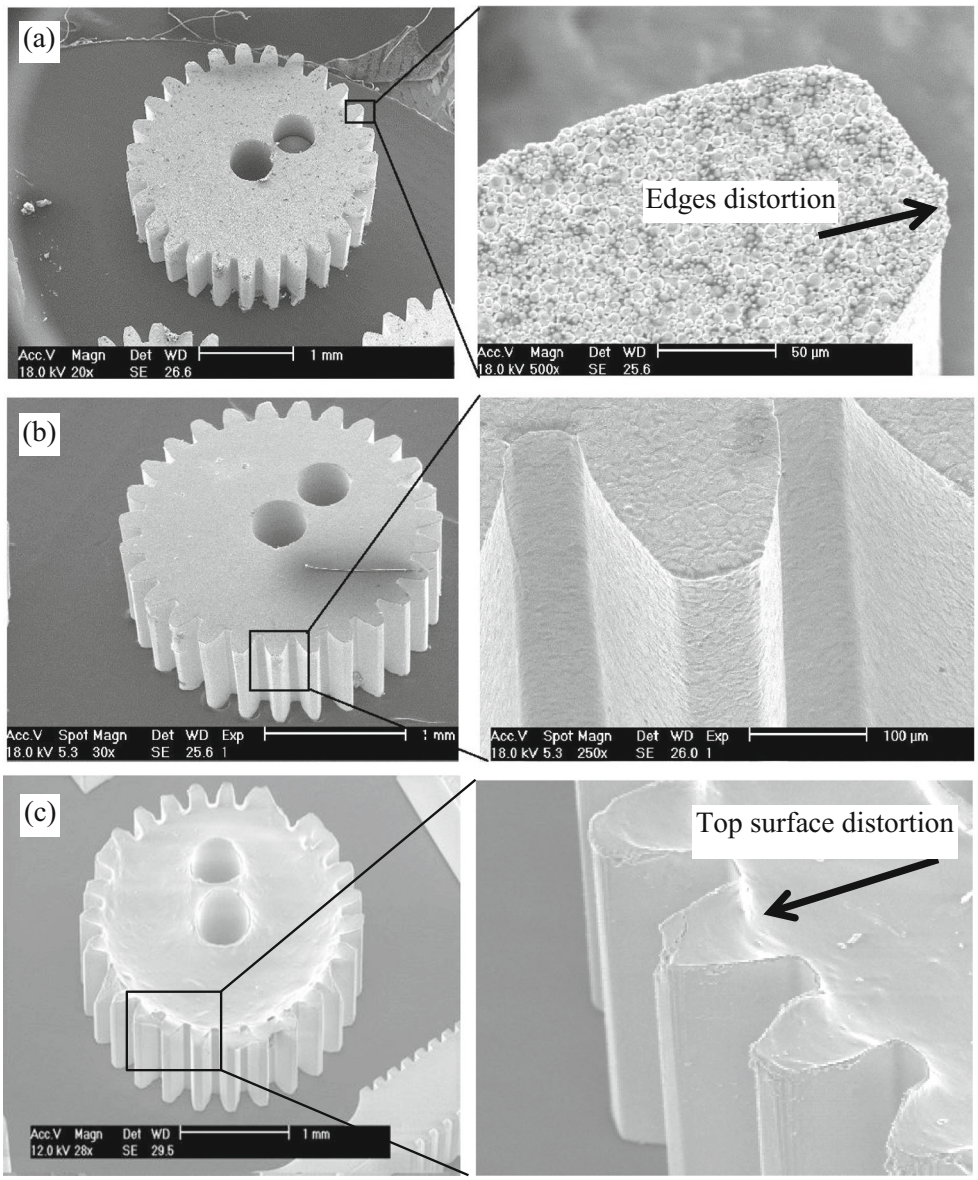

Fig. 3 Micro-gear with detailed micro-feature. **a** Green part after drying and de-moulding from soft mould, **b** sintered part in nitrogen/hydrogen mixture and **c** sintered part with the distorted top surface

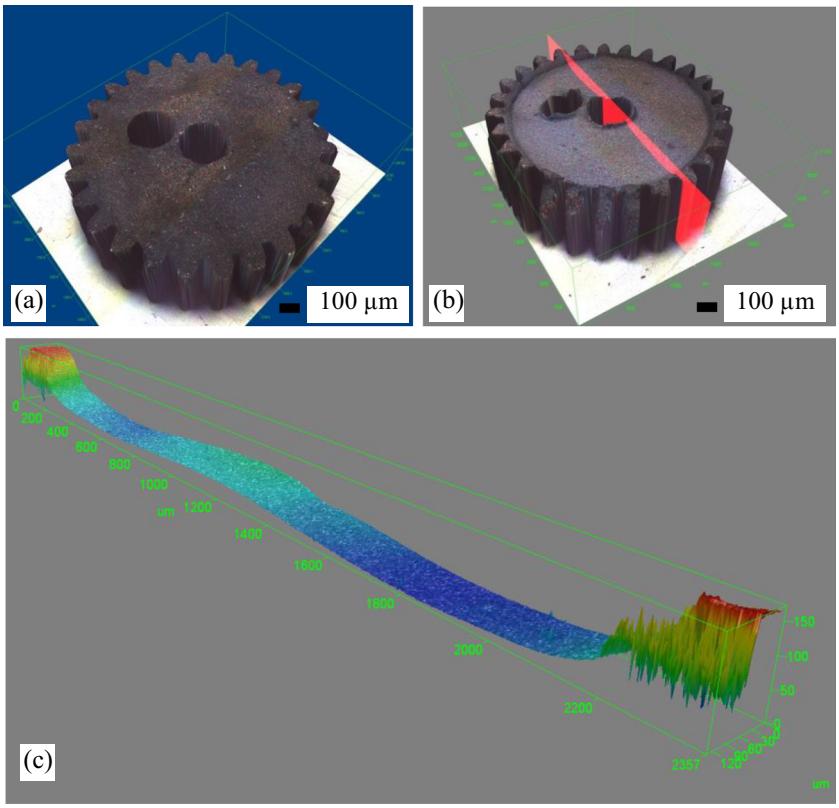

Fig. 4 The as-fabricated stainless steel micro-parts (sintered). **a** Confocal acquisition of the bottom surface, **b** confocal acquisition of the top surface and **c** section of the top surface

In this experiment, a mixture of acrylic polymer, Duramax B-1000 and B-1007 (Rohm and Haas), were used as binders. Also, Duramax D-3005 (Rohm and Haas, PA, USA), an ammonium salt of acrylic homopolymer, was used for dispersing the stainless steel powders. 0.1 g/ml Duramax D-3005 was added to distilled and mixed using an ultrasonic bath for 5 min. The stainless steel powder was added and stirred using a mechanical stirrer before adding the (B-1000+B-1007) binder (with 0.75 wt%) and re-stirring the whole mixture. Before use, the slurry was placed in a vacuum condition to get rid of

Table 2 The technological parameters adopted in µ-EDM machining

Operation	–	Roughing phase	First finishing	Second finishing
Regime	–	Roughing (long pulses)	Fine finishing (short pulses)	Fine finishing (short pulses)
Electrode polarity	pos/neg	neg	neg	neg
Width	[µs]	6.6	2	2
Frequency	[kHz]	90	180	180
Current	[index]	80	100	100
Maximum current peak value	[A]	30	1.15	1.15
Voltage	[V]	150	90	90
Gain	[index]	1000	230	230
Gap	[index]	60	74	74
Energy	[index]	365	13	13
Tool electrode type	–	Rod	Rod	Rod
Tool electrode material	–	Tungsten carbide	Tungsten carbide	Tungsten carbide
Tool electrode diameter	[mm]	0.4	0.4	0.4
Layer thickness	[mm]	0.0015	0.0009	0.0009
Total depth of machining	[mm]	0.07	0.05	0.045
Eroded volume	[mm3]	0.5537	0.3967	0.2901
Machining time	[s]	895	3994	4217

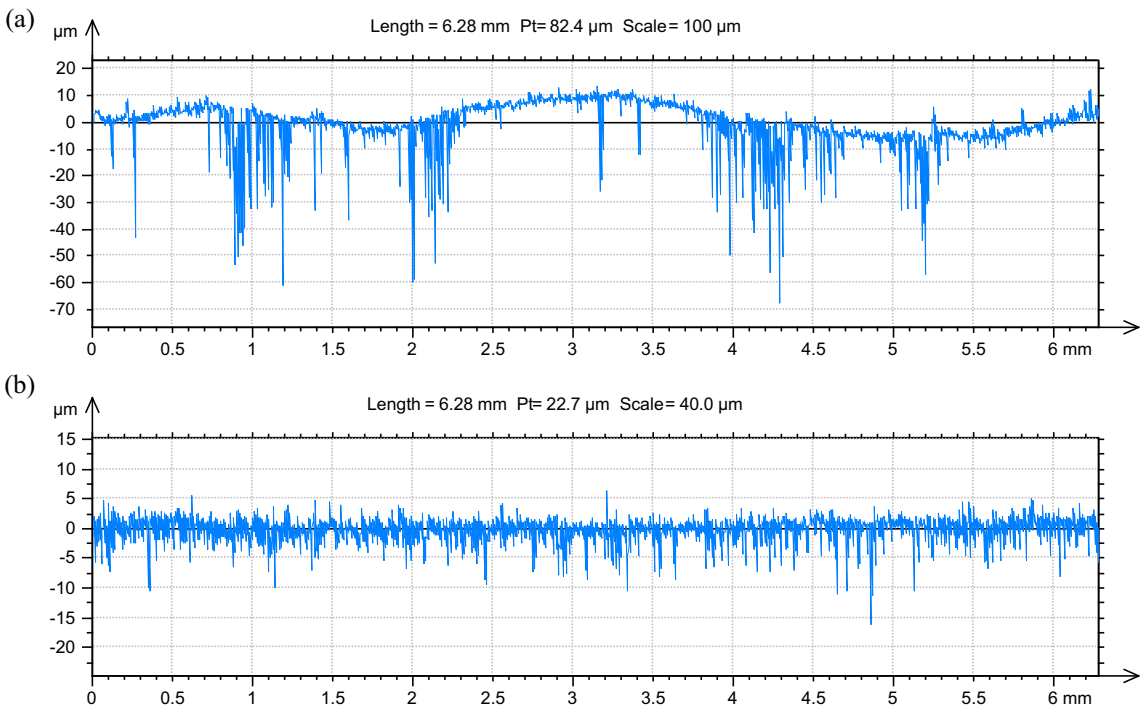

Fig. 5 Cross-section profiles of **a** the as-fabricated stainless steel micro-part (sintered). **b** The micro-machined samples after the second finishing process

any bubbles that could be entrapped during stirring. The cavities of the patterned PDMS moulds were filled up with the stainless steel slurry with the help aid of a vacuum to ensure the complete filling of all of the small features, as shown in Fig. 1c. Finally, the slurry was left to dry and the green component was extracted by carefully peeling off the soft PDMS moulds (Fig. 1d). After de-moulding, the green micro-parts were sintered, as shown in Fig. 1e, by being placed in a tube furnace which atmosphere consisted of 90 % nitrogen and 10 % hydrogen. The temperature increased gradually at a rate of 1.2 °C/min until reaching about 700 °C/min sufficient temperature for the both the binder and the dispersant to decompose. This was to prevent deformation during binder burn out. The green samples were held at 700 °C for 1 hour to ensure the complete burning out of the binder. Afterwards, the temperature was ramped up again to 1250 °C in the sintering stage at a rate of 5 °C/min and the samples were maintained at that temperature for 90 min before turning the furnace off and allowing the samples to cool inside the furnace to room temperature while maintaining the flow of the forming gas.

Finally, the developed micro-parts were micro-milled using a three-axis SARIX SX-200 µ-EDM (SARIX SA, Switzerland). See Fig. 1f, g. The EDM machine used is a three-axis machine, developed specifically for high precision and µ-EDM applications, as it is equipped with a relaxation-type generator enabling the discharge of very fine pulses (discharge energy down to few µJ). As combined with the CAM system, the automatic feeding of the electrode for the tool wear compensation in the *Z*-axis is also possible, thus allowing maximal flexibility in micro-milling operations. Negative polarity was applied through entire cutting operation, and hydrocarbon oil was used as dielectric. In the present work, the µ-EDM milling layer-by-layer approach has been adopted. In order to evaluate the performance of the µ-EDM process, surface topography of the samples has been characterized using an Axio CSM 700 confocal microscope from Carl Zeiss. The measures involved the evaluation of the overall shape and surface roughness (Ra) of the samples.

3 Results and discussions

The fabricated stainless micro-parts were first inspected using SEM to characterize the surface topography. Figure 3 shows the green and sintered stainless steel micro-gears and their detailed micro-features. It is clear that the green micro-gear has a distortion, specifically at the edges of the teeth. This is suggested to be because the de-moulding process was done manually. In addition, it can be seen that there are two distinct topologies of the top and bottom surfaces. The bottom surface of the micro-gear, shown in Fig. 3a, b, shows a good flatness, which is expected to be due to the good conformal between the slurry and the PDMS mould during drying. On the other hand, the top surface of the gear shows a convex profile (Fig. 3c). This is due to the difference in the evaporation rate between both sides. Obviously, the top surface, which was exposed to the air during drying, exhibited a higher drying rate than the bottom surface, resulting in such a distorted shape. The difference in the surface roughness of the top and bottom surfaces is shown in Fig. 4. It was found that, the

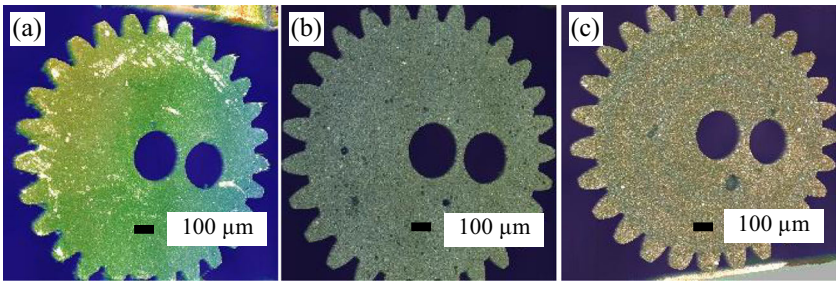

Fig. 6 Confocal acquisition images of the top surface after **a** roughing regime, **b** first finishing regime and **c** second finishing regime

measured surface roughness Ra of the top surface was 3.6 μm while it was 0.9 μm for the bottom surface. In addition, Fig. 4c shows a section of the top surface where the poor flatness is clearly highlighted.

The sample has been carefully clamped in order to avoid any damage during fixturing. By electric touches, the top surface of the sample is aligned to the surface of machine table. The erosion is performed adopting the micro-milling EDM layer-by-layer and following three steps:

1. Roughing phase of a depth of 0.07 mm using high energy level in order to obtain a planar surface of the sample.
2. An initial finishing phase of an additional depth of 0.05 mm using the lowest energy level has been performed.
3. A final finishing phase of a depth of 0.045 mm using the same lowest energy level has been carried out.

The two finishing phases have been executed in order to evaluate the sample homogeneity and its influence on the surface roughness. Table 2 summarizes the technological parameters adopted and the results obtained.

The surface roughness analysis has been performed adopting a low pass filter of 0.0025 mm and a high pass filter of 0.8 mm. Since the sample dimensions are small, the analysis considers a line length of 2 mm, shorter than the minimal length of 4 mm prescribed by the international standard. Since the sample dimensions did not permit to apply the international standard measurement of Ra, qualitative measures of this index are reported. The measurements were repeated after finishing the machining process. During the machining, a depth error control was carried out 40 times in order to have a better tool wear compensation.

The following cross-section profiles have been taken for the same part along a circle centered with the gear, see Fig. 5. Figure 5a shows the profile of the sample fabricated using soft lithography, while the Fig. 5b shows the same profile after the finishing operation by μ-EDM. By comparing the two profiles, it is evident the improvement in the flatness of the samples after using the optimized μ-EDM process.

A comparison of the surface topography of the micro-gears fabricated by soft lithography after being machined using μ-EDM operation is shown in Fig. 6. The resulting surfaces after the roughing, first and second finishing processes are shown in Fig. 6a–c, respectively. The micro-machining results indicated a significant improvement of the surface quality of the micro-gears via the application of μ-EDM. Surface roughness Ra of the top and bottom surfaces of the micro-gears has been improved from 3.4 and 0.9 μm, respectively, to 0.43 μm, for both surfaces, after the finishing operation. Using the finishing operations with low energy, a small layer thickness of 0.05 mm has been demonstrated to significantly improve the surface quality.

4 Conclusions

This research was carried out to cover the gap in producing high precision micro-components using soft lithography. It was aimed to develop stainless steel micro-implantable parts using hybrid soft lithography/μ-EDM process. Using soft lithography as one of the micro-fabrication techniques, stainless steel 316L micro-parts were fabricated. Surface roughness of the as-fabricated stainless steel micro-components has been significantly improved from Ra = 3.4 μm to Ra =0.43 μm using a μ-EDM milling technique. In addition, the cross-section profiles of the samples show that the flatness of the samples has been enhanced using the optimized μ-EDM process. It was also found that when the material is electro-conductive, μ-EDM process is a good choice for improving surface roughness and to machine sharp micro-features. In order to combine the two technologies, the definition of a common reference system for aligning the features produced by different process is required.

References

1. Gad-el-Hak M (2006) The MEMS handbook. CRC/Taylor & Francis, Florida
2. Goswami DY (2004) The CRC handbook of mechanical engineering. CRC Press
3. Marinis TF (2009) The future of microelectromechanical systems (MEMS). Strain 45:208–220
4. Brandner J (2012) Microfabrication in metals, ceramics and polymers. Russ J Gen Chem 82:2025–2033

5. Jiang L, Liu Z, Tang J, Zhang L, Shi K, Tian Z et al (2005) Three-dimensional micro-fabrication on copper and nickel. J Electroanal Chem 581:153–158
6. Arida H, Mohsen Q, Schöning M (2009) Microfabrication, characterization and analytical application of a new thin-film silver Microsensor. Electrochim Acta 54:3543–3547
7. Anthony R, Wang N, Casey DP, Mathúna CÓ, Rohan JF (2016) MEMS based fabrication of high-frequency integrated inductors on Ni–Cu–Zn ferrite substrates. J Magn Magn Mater 406:89–94
8. Imbaby M, Jiang K, Chang I (2008) Net shape fabrication of stainless-steel micro machine components from metallic powder. J Micromech Microeng 18:115018
9. Scholten K, Meng E (2015) Materials for microfabricated implantable devices: a review. Lab Chip 15:4256–4272
10. Lee CH, Kim Y. J., Jang J. H., and J. W. Park (2016) Modulating macrophage polarization with divalent cations in nanostructured titanium implant surfaces. Nanotechnology vol. 27
11. Shirkhorshidian A., Bishop N. C., Dominguez J., Grubbs R. K., Wendt J. R., Lilly M. P., *et al.* (2015) Transport spectroscopy of low disorder silicon tunnel barriers with and without Sb implants. Nanotechnology vol. 26
12. Imbaby M, Ostadi H, Jiang K (2009) Characterisation of stainless steel microparts fabricated by soft moulding technique. Micro & Nano Letters 4(2):99–105
13. Imbaby M, Jiang K, Chang I (2008) Fabrication of 316-L stainless steel micro parts by softlithography and powder metallurgy. Mater Lett 62:4213–4216
14. Qin Y, Brockett A, Ma Y, Razali A, Zhao J, Harrison C et al (2010) Micro-manufacturing: research, technology outcomes and development issues. Int J Adv Manuf Technol 47:821–837
15. Jackman RJ, Brittain ST, Adams A, Wu H, Prentiss MG, Whitesides S et al (1999) Three-dimensional metallic microstructures fabricated by soft lithography and microelectrodeposition. Langmuir 15:826–836
16. Xu B, Wu X-y, Ling S-q, Luo F, Du C-l, Sun X-q (2013) Fabrication of 3D metal micro-mold based on femtosecond laser cutting and micro-electric resistance slip welding. Int J Adv Manuf Technol 66:601–609
17. Vaezi M, Seitz H, Yang S (2013) A review on 3D micro-additive manufacturing technologies. Int J Adv Manuf Technol 67:1721–1754
18. Shyu RF, Yang H (2006) Vacuum suction aid for microlens array formation using LIGA-like process. Int J Adv Manuf Technol 29: 518–523
19. Imbaby M, Jiang K (2010) Micro fabrication of stainless steel micro components using soft moulding and aqueous slurry. Microelectron Eng 87:72–78
20. Xia Y, Whitesides GM (1998) Soft lithography. Annu Rev Mater Sci 28:153–184
21. Zhu Z, Hassanin H, Jiang K (2010) A soft moulding process for manufacture of net-shape ceramic microcomponents. Int J Adv Manuf Technol 47:147–152
22. Hassanin H, Jiang K (2013) Effects of particle size on soft lithography process, the green and sintered micro alumina parts. Int J Appl Ceram Technol 10:1014–1022
23. Schönholzer UP, Gauckler LJ (1999) Ceramic parts patterned in the micrometer range. Adv Mater 11:630–632
24. Kim J-S, Jiang K, Chang I (2006) A net shape process for metallic microcomponent fabrication using Al and Cu micro/nano powders. J Micromech Microeng 16:48
25. Zhu Z, Wei X, Jiang K (2007) A net-shape fabrication process of alumina micro-components using a soft lithography technique. J Micromech Microeng 17:193
26. Kahraman M, Daggumati P, Kurtulus O, Seker E, Wachsmann-Hogiu S (2013) Fabrication and characterization of flexible and tunable plasmonic nanostructures. Sci Rep 3:3396
27. Rogers JA, Paul KE, Whitesides GM (1998) Quantifying distortions in soft lithography. J Vac Sci Technol B 16:88–97
28. Martin CR, Aksay IA (2005) Microchannel molding: a soft lithography-inspired approach to micrometer-scale patterning. J Mater Res 20:1995–2003
29. Hassanin H, Jiang K (2013) Fabrication and characterization of stabilised zirconia micro parts via slip casting and soft moulding. Scr Mater 69:433–436
30. Liu K, Lauwers B, Reynaerts D (2010) Process capabilities of micro-EDM and its applications. Int J Adv Manuf Technol 47: 11–19
31. Mahendran RDS, Nagarajan T, Majdi A (2010) A review of micro-EDM. In: Proceedings of the International MultiConference of Engineers and Computer Scientists (IMECS 2010), Hong Kong
32. Hassanin H, Modica F, El-Sayed MA, Liu J, Essa K (2016) Manufacturing of Ti–6Al–4V micro-implantable parts using hybrid selective laser melting and micro-electrical discharge machining. Adv Eng Mater 18:1544–1549
33. Tiwary AP, Pradhan BB, Bhattacharyya B (2015) Study on the influence of micro-EDM process parameters during machining of Ti–6Al–4V superalloy. Int J Adv Manuf Technol 76:151–160
34. Maradia U, Scuderi M, Knaak R, Boccadoro M, Beltrami I, Stirnimann J et al (2013) Super-finished surfaces using meso-micro EDM. Procedia CIRP 6:157–162
35. Rees A, Brousseau E, Dimov SS, Bigot S, Griffiths CA (2013) Development of surface roughness optimisation and prediction for the process of wire electro-discharge grinding. Int J Adv Manuf Technol 64:1395–1410
36. Ay M, Çaydaş U, Hasçalık A (2013) Optimization of micro-EDM drilling of inconel 718 superalloy. Int J Adv Manuf Technol 66: 1015–1023
37. Luo YF, Zhang ZY, Yu CY, Zhang YZ (1988) Mirror surface EDM by electric field partially induced. CIRP Ann Manuf Technol 37: 179–181